

Soret and Dufour effects on MHD mixed convective heat and mass transfer flow with thermophoresis past a vertical flat plate embedded in a saturated porous medium in the presence of radiation and viscous dissipation

S. Jagadha¹ and Naikoti Kishan²

¹Department of Mathematics, St. Martin's Engineering College, Dhullapally, Secunderabad, Telangana, India

²Department of Mathematics, University College of Science, Osmania University, Hyderabad, India

ABSTRACT

The effects of Soret and Dufour and MHD on Darcy-Forchheimer mixed convection flow with heat and mass transfer from a vertical flat plate embedded in a saturated porous medium taking into the influence thermophoresis, viscous dissipation and radiation. The fluid is considered in a grey medium and the Rosseland approximation is used to describe the radiative heat flux in the energy equation. A similarity solution for the transformed governing equations is obtained. The coupled non-linear ordinary equations are linearized by using Quasi-linearization technique. The governing coupled ordinary differential equations are being solved by employing an implicit finite difference scheme. Numerical computation are carried out for the non dimensional physical parameters. The results are analyzed for the effect of different physical parameters, such as radiation R , Soret number S_r , Dufour D_f , Viscous dissipation Ec , mixed convection parameter Ra_x/Pe_x , buoyancy ratio N , inertia parameter Λ , magnetic field parameter Ha , Prandtl number Pr , Lewis number Le , Schmidt number Sc and thermophoretic parameter τ .

Keywords: Soret and Dufour, Darcy-Forchheimer, Radiation, MHD, Finite difference method and mixed convection.

INTRODUCTION

Mixed convective heat and mass transfer flow is very important in manufacturing industries for the design of reliable equipment, nuclear plants, gas turbines, and various propulsion devices for aircraft, missiles, satellites, and space vehicles. In light of these various applications, the unsteady MHD combined convection over a moving vertical sheet in a fluid saturated porous medium with uniform surface heat flux was studied by El-Kabeira *et.al* [1]. Mixed convection on bodies embedded in a non-Darcian porous medium have been extensively studied and reported for flow driven by temperature variations only [2,3,4,5,]. The problem of Darcy-Forchheimer mixed convection heat and mass transfer in fluid-saturated porous media was studied by Rami *et al.* [6]. Goren [7] was one of the first to study the role of thermophoresis in the laminar flow of a viscous and incompressible fluid. Most previous studies of the same problem neglected viscous dissipation and thermophoresis. But Gebhart [8] has shown that the viscous dissipation effect plays an important role in natural convection in various devices that are subjected to large variations of gravitational force or that operate at high rotational speeds. Motivated by the above investigations and possible applications.

Small particles, such as dust, when suspended in a gaseous medium possessing a temperature gradient, it will move in the direction opposite to the temperature gradient. This motion is known as thermophoresis, occurs because gas

molecules colliding on one side of particle have different average velocities from those on the other side due to the temperature gradient. The studies in aerosol deposition have become more and more important for engineering applications. The factors that influence particle deposition include convection, Brownian diffusion, sedimentation, inertial effect, thermophoresis and surface geometry, respectively. Aerosol particles are likely to be generated during a severe core melt accident at a nuclear power plant. If these particles strike and attach to the walls of the heat exchanger, they can impair heat transfer and lead to potentially high temperatures and pressures. The force experienced by a small aerosol particle in the presence of a temperature gradient is known as the thermophoretic force. This phenomenon has been the subject of considerable study in the past. Goldsmith and May [9] first studied the thermophoretic transport involved in a simple one-dimensional flow for the measurement of the thermophoretic velocity. Selim *et al.* [10] studied the effect of surface mass flux on mixed convective flow past a heated vertical flat permeable plate with thermophoresis. Chamkha and Pop looked to the effect of thermophoresis particle deposition in free convection boundary layer from a vertical flat plate embedded in a porous medium; the steady free convection over an isothermal vertical circular cylinder embedded in a fluid-saturated porous medium in the presence of the thermophoresis particle deposition effect was analyzed by Chamka *et al.* [11]. Hossain and Takhar [12] analyzed the effect of radiation using the Rosseland diffusion approximation on mixed convection along a vertical plate with uniform free stream velocity and surface temperature. Damesh *et al.* [13] studied the effect of radiation and heat transfer in different geometry for various flow conditions.

The Dufour and Soret effects were neglected in many reported research studies, since they are of a smaller order of magnitude than the effects described by Fourier's and Fick's laws. The energy flux can be generated by the temperature gradients and the composition gradients. The mass transfer caused by the temperature gradient is called the Soret effect, while the heat transfer caused by the concentration gradient is called the Dufour effect. However, such effects become crucial when the density difference exists in the flow regimes. The Soret effect, for instance, has been utilized for isotope separation. In a mixture between gases with very light molecular weight (He, H₂) and medium molecular weight (N₂, air), the Dufour effect was found to be of considerable magnitude such that it cannot be neglected (Eckert and Drak [14]). The Dufour and Soret effects were studied by many researchers. Eldabe *et al.* [15], studied the flow in boundary layer effects. D. Srinivasacharya *et al.* [16] presented the effect of Soret and Dufour on mixed convection in a non-Darcy porous medium saturated with micropolar fluid.

Most previous applications Kishan and Srinivas [17] studied the influence of MHD on mixed convection flow, heat and mass transfer along a vertical flat plate embedded in a fluid saturated porous medium with the viscous dissipation and thermophoresis effects.

The aim of the present investigation of the simultaneous effects of Soret and Dufour of MHD mixed convection flow with heat and mass transfer over a vertical porous plate embedded in a saturated porous medium subject to a thermal radiation and viscous dissipation. The governing coupled equations are solved by using implicit finite difference scheme with C-programming code.

MATHEMATICAL FORMULATION

We consider the steady flow of an incompressible viscous, radiating, hydromagnetic fluid bounded by a vertical flat plate embedded in a fluid-saturated porous medium. The x-coordinate is measured along the plate from its leading edge and the y-coordinate is normal to it. Assumed the fluid to be Newtonian, electrically conductive, wall temperature as T_w and concentration as C_w which is embedded in a fluid saturated porous medium of ambient temperature T_∞ and concentration C_∞ , where $T_w > T_\infty$ and $C_w > C_\infty$ respectively. The density variations and the effects of buoyancy are taken into account in the momentum equation (Boussinesq approximation [18]) and the Rosseland approximation [19] is used to describe the radiative heat flux in the energy equation. A uniform transverse magnetic field of strength β_0 is applied parallel to the y axis. Under the above assumption, the governing equation for this problem can be written as:

$$\frac{\partial u}{\partial x} + \frac{\partial v}{\partial y} = 0 \quad (1)$$

$$\left[1 + \frac{\sigma \beta_0^2 k}{\rho \nu}\right] \frac{\partial u}{\partial y} + \frac{c_f \sqrt{K_1}}{\nu} \frac{\partial (u^2)}{\partial y} = \pm \frac{K_1 g}{\nu} \left[\beta_T \frac{\partial T}{\partial y} + \beta_C \frac{\partial C}{\partial y}\right] \quad (2)$$

$$u \frac{\partial T}{\partial x} + v \frac{\partial T}{\partial y} = \alpha_m \frac{\partial^2 T}{\partial y^2} + \frac{\nu}{c_p} \left(\frac{\partial u}{\partial y}\right)^2 - \frac{1}{\rho c_p} \frac{\partial q_r}{\partial y} + \frac{D_m K_T}{c_s c_p} \frac{\partial^2 C}{\partial y^2} \quad (3)$$

$$u \frac{\partial C}{\partial x} + v \frac{\partial C}{\partial y} = D_m \frac{\partial^2 C}{\partial y^2} - \frac{\partial}{\partial y}(V_T C) + \frac{D_m K_T}{T_m} \frac{\partial^2 T}{\partial y^2} \quad (4)$$

The boundary conditions are given by

$$\begin{aligned} v = 0, \quad T = T_w, \quad C = C_w \quad \text{as } y = 0 \\ u = u_\infty, \quad T = T_\infty, \quad C = C_\infty \quad \text{as } y \rightarrow \infty \end{aligned} \quad (5)$$

Where u and v are the velocity components along the x and y directions, respectively, T and C are, respectively, the temperature and the concentration, c_f is the Forchheimer coefficient, K_l is the Darcy permeability, g is the acceleration due to gravity, ν is the kinematic viscosity, β_T is the coefficient of thermal expansion, β_C is the coefficient of concentration expansion, α_m is the thermal diffusivity of the fluid-saturated porous medium, c_p is the specific heat of the fluid at constant pressure, q_r is the radiative heat flux and D_m is the mass diffusivity. In Eq. (2), the plus sign corresponds to the case where the buoyancy force has a component "aiding" the forced flow, and the minus sign refers to the "opposing" case. By using the Rosseland approximation for radiation [20] and following Raptis [21], the radiative heat flux q_r is given by

$$q_r = \frac{-16\sigma_1 T_\infty^3}{3k_e} \frac{\partial T}{\partial y} \quad (6)$$

where σ_1 is the Stefan-Boltzmann constant, k_e the mean absorption coefficient and T_∞ the temperature of the ambient fluid. With using Eq. (6) and Eq. (3) gives

$$u \frac{\partial T}{\partial x} + v \frac{\partial T}{\partial y} = \alpha \frac{\partial^2 T}{\partial y^2} + \frac{\nu}{c_p} \left(\frac{\partial u}{\partial y} \right)^2 - \frac{16\sigma_1 T_\infty^3}{3\rho c_p k_e} \frac{\partial^2 T}{\partial y^2} + \frac{D_m K_T}{c_s c_p} \frac{\partial^2 C}{\partial y^2} \quad (7)$$

Now we define the following dimensionless variables for mixed convection:

$$\begin{aligned} \eta = \sqrt{Pe_x} \frac{y}{x}, \quad \psi = \alpha \sqrt{Pe_x} f(\eta), \\ \theta(\eta) = (T - T_\infty)/(T_w - T_\infty), \\ \phi(\eta) = (C - C_\infty)/(C_w - C_\infty) \end{aligned} \quad (8)$$

Where ψ is the stream function that satisfies the continuity equation and η is the dimensionless similarity variable. With these changes of variables, Eq. (1) is identically satisfied and Eqs. (2), (4) and (7) are transformed to

$$(1 + Ha^2)f'' + 2\Lambda f' f'' = \pm \left(\frac{Ra_x}{Pe_x} \right) (\theta' + N\phi') \quad (9)$$

$$\theta'' \left(1 + \frac{4}{3R} \right) + \frac{1}{2} f \theta' + Pr Ec f''^2 + D_f \phi'' = 0 \quad (10)$$

$$\phi'' + \frac{1}{2} Le f \phi' - \tau Sc (\theta' \phi' + \phi \theta'') + Le Sr \theta'' = 0 \quad (11)$$

The corresponding boundary conditions take the form

$$\begin{aligned} f(\eta) = 0, \quad \theta(\eta) = 1, \quad \phi(\eta) = 1 \quad \text{on } \eta = 0 \\ f'(\eta) \rightarrow 1, \quad \theta(\eta) \rightarrow 0, \quad \phi(\eta) \rightarrow 0 \quad \text{as } \eta \rightarrow \infty \end{aligned} \quad (12)$$

Where the primes denote differentiation with respect to η , $Sc = \nu/D_m$ is the Schmidt number, $N = \beta_c(C_w - C_\infty)/\beta_T(T_w - T_\infty)$ is the buoyancy ratio parameter, $Ra_x = (K_1 g \beta_T)(T_w - T_\infty)x/\alpha\nu$ is the thermal Rayleigh number, $Pe_x = u_\infty x/\alpha_m$ is the local Peclet number, $\Lambda = c_f \sqrt{K_1} u_\infty/\nu$ is the inertia parameter, $Ha^2 = \sigma \beta_o^2 k/\rho\nu$ is the magnetic parameter, $R = k k_e/4\sigma_1 T_\infty^3$ is the radiation parameter (k is the thermal conductivity) and $Le = \alpha_m/D_m$ is the Lewis number, $Ec = u_\infty^2/c_p(T_w - T_\infty)$ is the Eckert number, $D_f = D_m k_T(C_w - C_\infty)/\alpha_m c_s c_p(T_w - T_\infty)$ is the Dufour number and the Sore number is $S_r = D_m k_T(T_w - T_\infty)/\alpha_m T_m(C_\infty - C_\infty)$

3. NUMERICAL SOLUTIONS

In order to get physical insight, we integrate the system of ordinary differential equations, Eqs.(9)-(11), with the boundary conditions in Eq. (12) numerically by means of implicit finite difference method. Applying the Quasi-linearization technique, Bellman and Kalaba [22] to the non-linear equation (9) we obtain as

$$(1 + Ha^2 + 2 \lambda F')f'' + 2 \lambda F'' f' = \pm \left(\frac{Ra_x}{Pe_x}\right) (\theta' + N\phi') + 2 \lambda F'' F' \quad (13)$$

Where assumed F is the value of f at n^{th} iteration and f is at $(n+1)^{\text{th}}$ iteration. The convergence criterion is fixed as $|F - f| < 10^{-5}$

Using an implicit finite difference scheme for the equation (13),(10) and (11), we obtain

$$a[i]f[i-1] + b[i]f[i] + c[i]f[i+1] = d[i] \quad (14)$$

$$a_1[i]\theta[i-1] + b_1[i]\theta[i] + c_1[i]\theta[i+1] = d_1[i] \quad (15)$$

$$a_2[i]\phi[i-1] + b_2[i]\phi[i] + c_2[i]\phi[i+1] = d_2[i] \quad (16)$$

where

$$a[i] = 1 + Ha^2 + 2 \lambda F_1[i] - 0.5 * h * 2 \lambda F_2[i]$$

$$b[i] = -2 * (1 + Ha^2 + 2 \lambda F_1[i])$$

$$c[i] = 1 + Ha^2 + 2 \lambda F_1[i] + 0.5 * h * 2 \lambda F_2[i]$$

$$d[i] = h * h * \pm \left(\frac{Ra_x}{Pe_x}\right) (\theta_1 + N\phi_1) + 2 \lambda F_2[i] F_1[i]$$

$$a_1[i] = 1 + (4/3R) - 0.5 * h * 0.5 * f[i]$$

$$b_1[i] = -2 * (1 + (4/3R))$$

$$c_1[i] = 1 + (4/3R) + 0.5 * h * 0.5 * f[i]$$

$$d_1[i] = h * h * - Pr Ec f_2[i] * f_2[i] - D_f \phi_2[i]$$

$$a_2[i] = 1 - 0.5 * h * (0.5 * f[i] * Le - \tau Sc \theta_1[i])$$

$$b_2[i] = -2 - h * h * \tau Sc \theta_2[i]$$

$$c_2[i] = 1 + 0.5 * h * (0.5 * f[i] * Le - \tau Sc \theta_1[i])$$

$$d_2[i] = h * h * - Le S \theta_2[i] \quad \text{and}$$

$$A[i] = 1 + Ha^2 + 2 \lambda F_1[i]$$

$$B[i] = 2 \lambda F_2[i]$$

$$D[i] = \pm \left(\frac{Ra_x}{Pe_x}\right) (\theta_1 + N\phi_1) + 2 \lambda F_2[i] F_1[i]$$

$$A_1[i] = 1 + (4/3R)$$

$$B_1[i] = 0.5 * f[i]$$

$$D_1[i] = - Pr Ec f_2[i] * f_2[i] - D_f \phi_2[i]$$

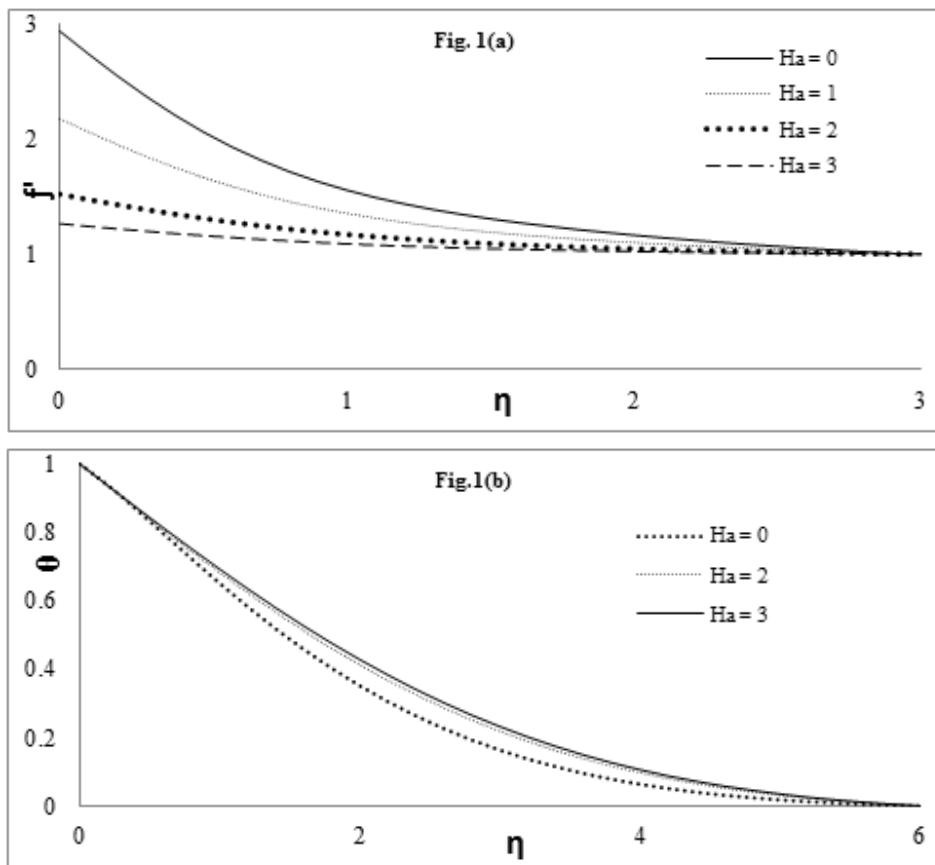
$$A_2[i] = 1, \quad B_2[i] = 0.5 * f[i] * Le - \tau Sc \theta_1[i],$$

$$C_2[i] = -\tau Sc \theta_2[i] \quad D_2[i] = -Le S_r \theta_2[i]$$

The set of equations (14)-(16) are coupled equations, which are solved by using the Gauss Seidel iteration method by using the C-programming code. The iterative procedure is initiated by the solution of concentration equation followed by energy equation and momentum equation which is continued until convergence is achieved. To get a converged solution and it was set to 10^{-5} for dependent variable f' , θ , ϕ .

RESULTS AND DISCUSSION

The governing boundary layer equations (1)-(4) are coupled non-linear partial differential equations be solved under the boundary conditions (5). However, exact or approximate solutions are not possible for this set of equations. Hence the coupled non-linear partial equations are transformed to ordinary differential equations by using the similarity transformation. To linearize the non-linear ordinary differential equations we used the Quasi-linearization technique[22]. The linearized coupled ordinary differential equations (9)-(11) with boundary conditions (12) are solved by using the implicit finite difference method.



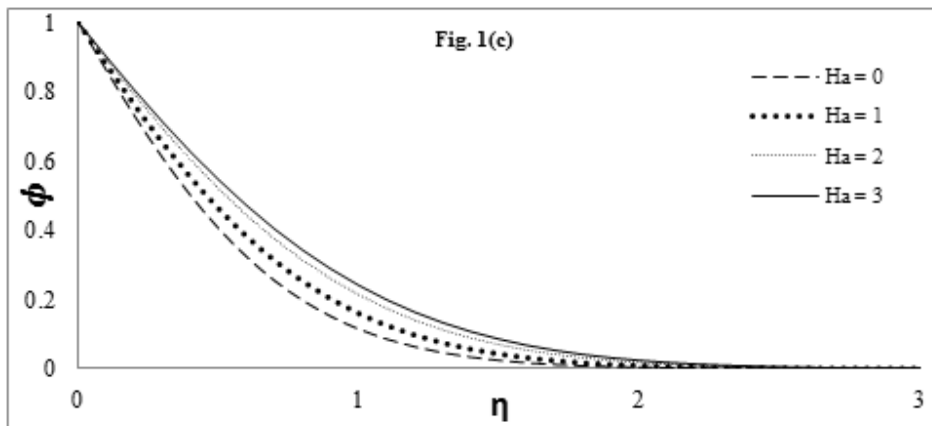
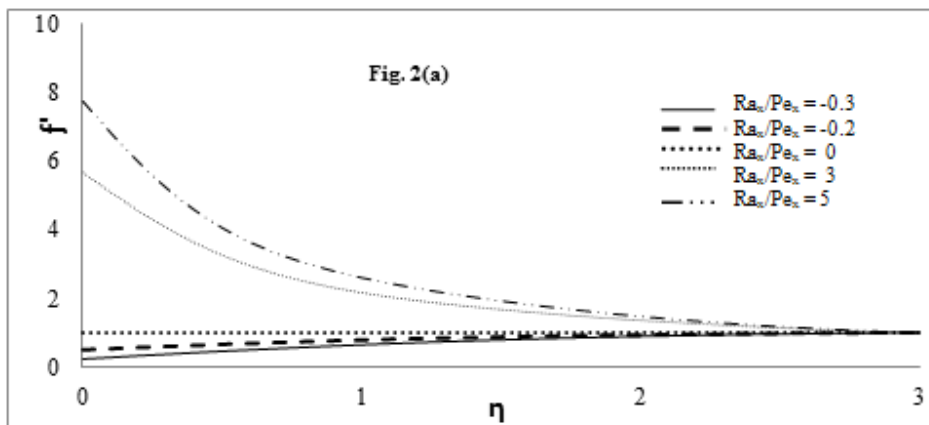


Fig. 1 Effects of magnetic parameter Ha for $Ra_x/Pe_x=1, R=0.5, \Lambda=0.1, Pr=0.73, Le=2, S_r=2, D_f=0.03, Sc=1, \tau=0.5, N=2, Ec=0.5$ on (a) Velocity profile (b) Temperature profile (c) Concentration profile

The computations have been carried for various values of magnetic parameter Ha, mixed convection parameter Ra_x/Pe_x , radiation parameter R, inertia parameter Λ , Prandtl number Pr, Lewis number Le, Soret number S_r , Dufour number D_f , Schmidt number Sc, thermophoretic number τ and buoyancy ratio parameter N. In addition, the edge of the boundary layer $\eta \rightarrow \infty$ was approximated by $\eta_{max} = 6$, which was sufficiently large for velocity to approach the relevant stream velocity. In order to illustrate the results graphically, the numerical values are plotted in figures 1 to 10. These figures depict the velocity profile, temperature profile and concentration profiles. The values of Prandtl number Pr are chosen $Pr=0.73$ which corresponds to air. The values of other parameters fixed as $Ra_x/Pe_x=1, R=0.5, \Lambda=0.1, Ec=0.5, Pr=0.73, Le=2, S_r=2, D_f=0.03, Sc=1, \tau=0.5, N=2$. Fig.1 reference the effect of magnetic parameter Ha on the velocity, temperature and concentration profiles. It is evident from the figure the velocity profile f' decreases with the increase of magnetic parameter Ha. The temperature and concentration profiles increase with the increase of magnetic parameter Ha. It is because that applications of transverse magnetic field will result a resistive type of force (Lorentz force) similar to drag force which tends to resist the fluid flow and thus reducing its velocity.



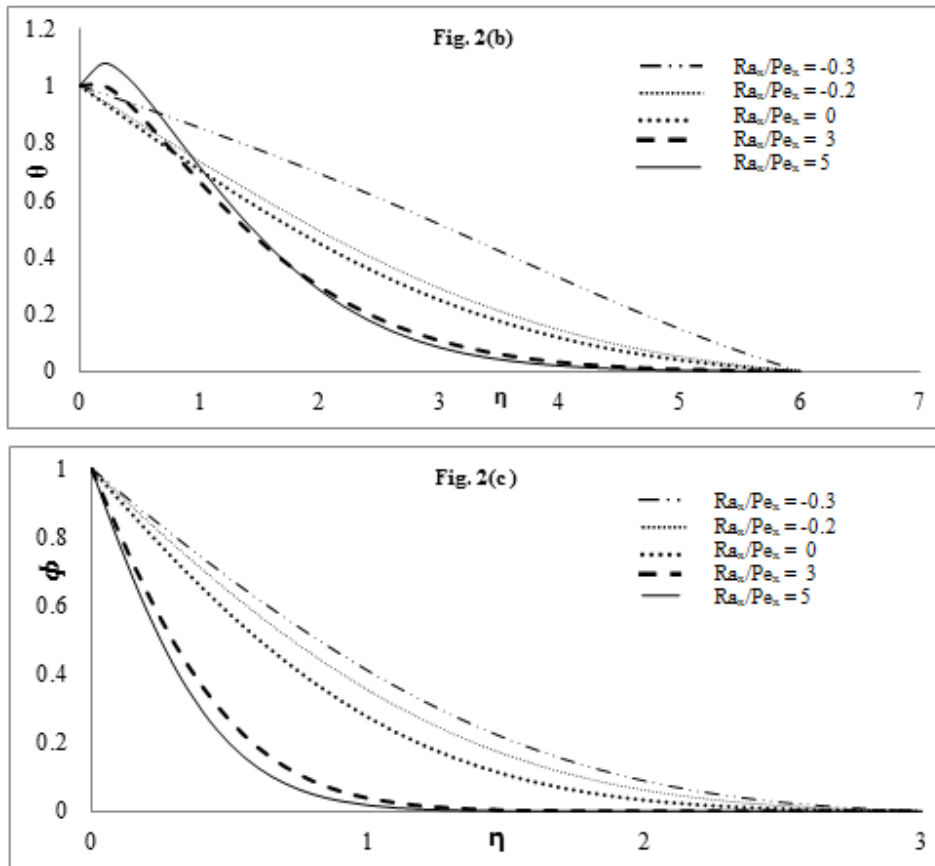
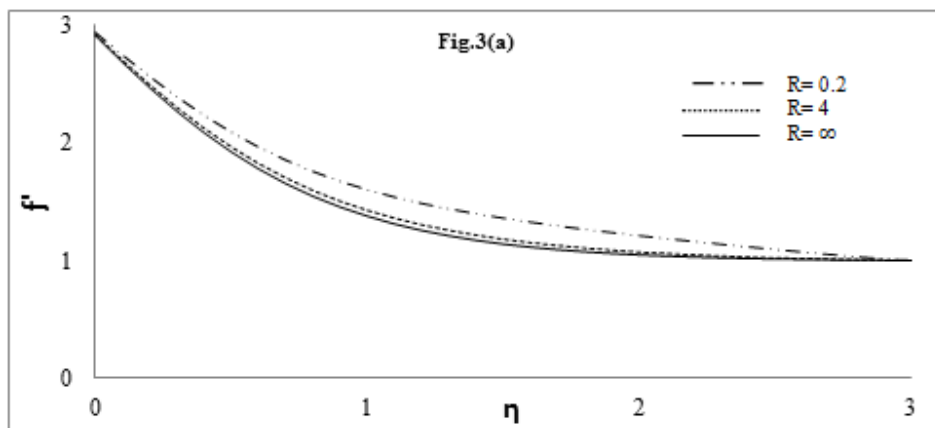


Fig.2 Effects of mixed parameter Ra_w/Pe_w for $\Lambda = 0.1, R = 0.5, N = 2, Pr = 0.73, Le = 2, S_r = 2, D_r = 0.03, Sc = 1, \tau = 0.5, Ha = 0, Ec = 0.5$ on (a) Velocity profile (b) Temperature profile (c) concentration profile



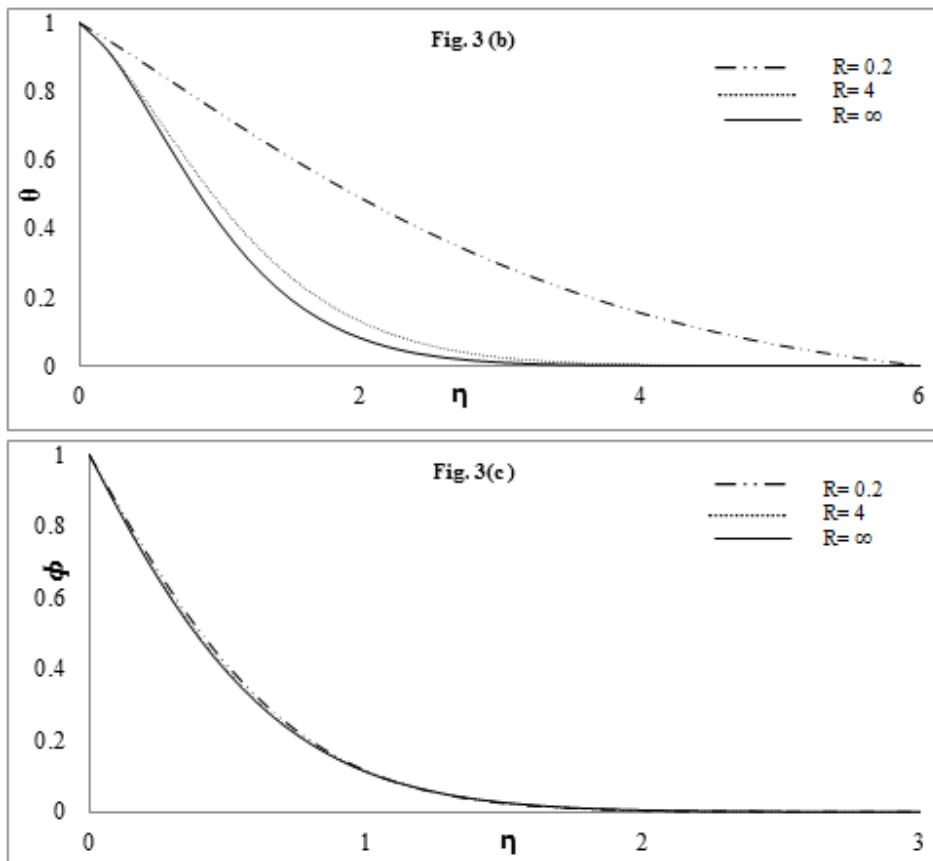
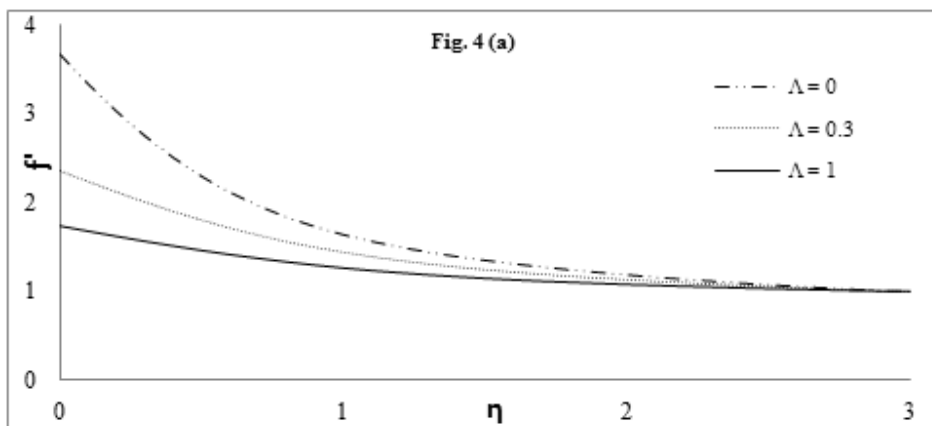


Fig. 3 Effects of Radiation parameter R for $\Lambda = 0.1$, $Ra_x/Pe_x = 1$, $N = 2$, $Pr = 0.73$, $Le = 2$, $S_r = 2$, $D_f = 0.03$, $Sc = 1$, $\tau = 0.5$, $Ha = 0$ and $Ec = 0.5$ on (a) Velocity profile (b) Temperature profile (c) Concentration profile

Figure (2) illustrates the influence of the mixed convection parameter Ra_x/Pe_x on velocity, temperature and concentration profiles respectively. In fact, the mixed convection parameter Ra_x/Pe_x is chosen as $Ra_x/Pe_x \gg 1$ flow is dominated by natural convection whereas $Ra_x/Pe_x \ll 1$ the flow is leading forced convection when $Ra_x/Pe_x = 1$, the effects of natural and forced convection are of equal importance, and the flow is truly under mixed convection. From fig.(2) it is noticed that with the increasing Ra_x/Pe_x , the velocity profile f' increase while temperature and concentration profiles decreases.



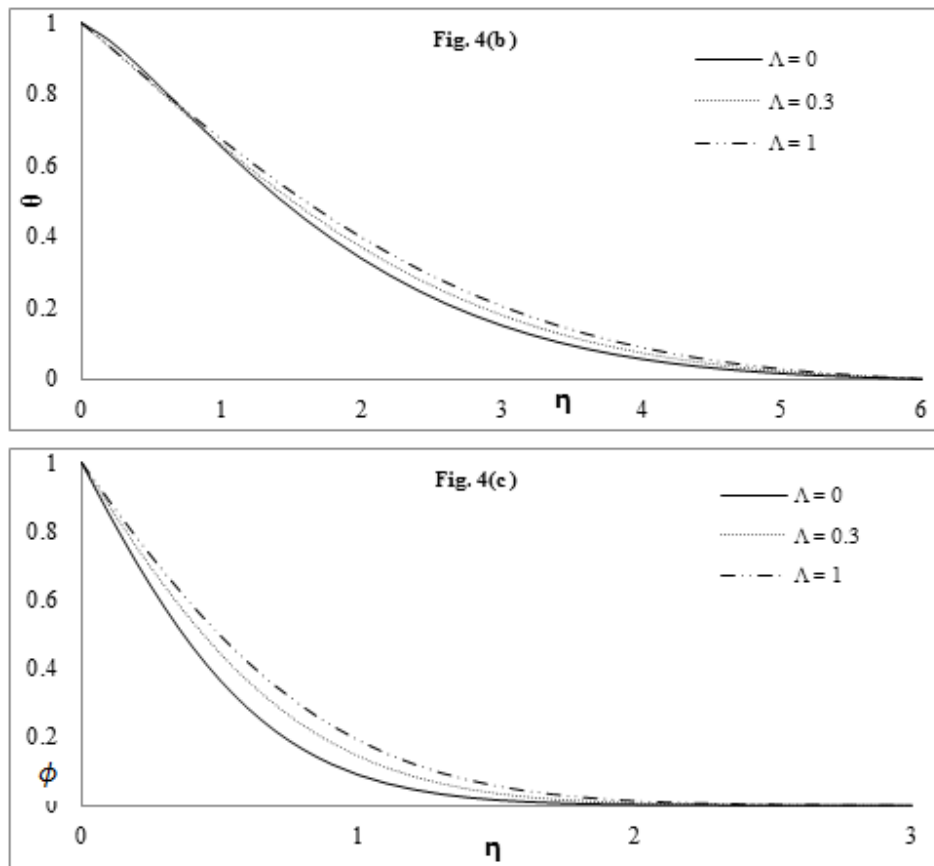


Fig. 4 Effects of inertia parameter Λ for $Ra_x/Pe_x=1$, $F = 0.5$, $N = 2$, $Pr = 0.73$, $Le = 2$, $S_r = 2$, $D_f = 0.03$, $Sc = 1$, $\tau = 0.5$, $Ha = 0$ and $Ec=0.5$ (a) Velocity profile (b) Temperature profile (c) Concentration profile

Figure (3) is drawn for the effects of Radiation parameter R on velocity, temperature and concentration profiles. An increase in the radiation parameter R leads to decrease the velocity profiles f' , temperature profiles θ within the boundary layer as well as thickness of the velocity and temperature boundary layer. This is because for large value of radiation parameter corresponds to an increased dominance of conduction over radiation, thereby decreasing buoyancy force and the thickness of the thermal and the momentum boundary layers. The effect of radiation parameter R is very meagre on concentration profile.

Figure (4) depicts the effect of inertia parameter Λ on velocity, temperature and concentration profiles. As shown in the figure the velocity profile decrease with increasing inertia parameter Λ , whereas temperature and concentration profiles increases.

The effect of buoyancy ratio parameter N is shown in figure(5) It is found from figure 5(a) the velocity profile f' increases with increasing the buoyancy ratio parameter N , while the temperature and concentration profiles decreases with the effect of N is observed from figures 5(b) and 5(c). This is because the effect of buoyancy ratio N is to increase the surface heat and mass transfer rates. It can be observed from figure (6) the velocity distribution f' and concentration profile ϕ decreases with the increasing of thermophoretic parameter τ .

The effect of Soret and Dufour is shown in figure (7). From figure 7(a) and 7(b) the velocity and temperature profiles increase with the increase of Dufour number (or decrease of Soret number) whereas reverse phenomena is observed in concentration profile showed in fig.7(c).

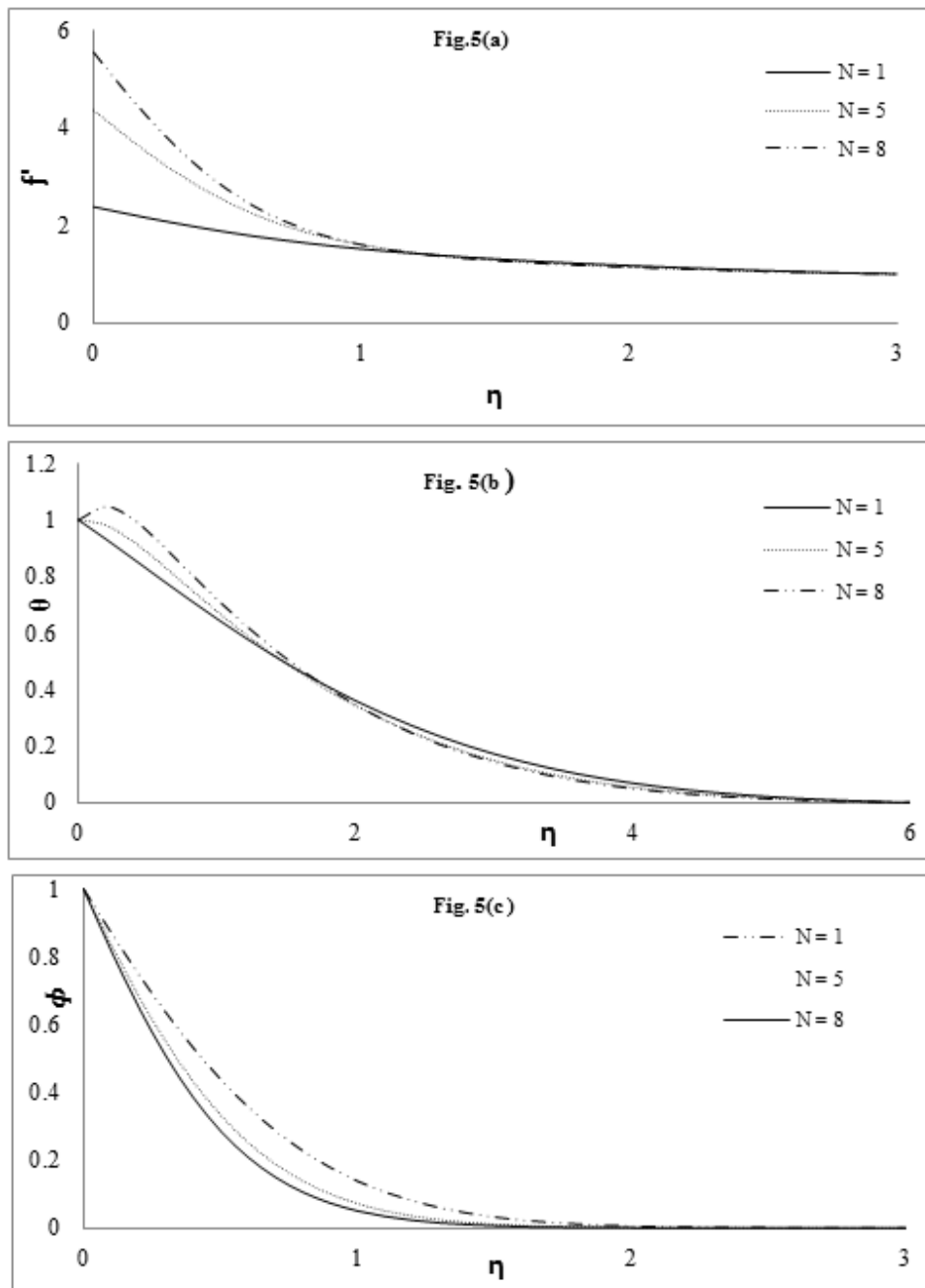


Fig.5 Effects of buoyancy ratio parameter N for $Ra_v/Pe_x = 1, F = 0.5, \Lambda = 0.1, Pr = 0.73, Le = 2, S_r = 2, D_f = 0.03, Sc = 1, \tau = 0.5, Ha = 0$ and $Ec = 0.5$ on (a) Velocity profile (b) Temperature profile (c) Concentration profile

The effect of Lewis number Le for the velocity and concentration profile inside the boundary layer region displayed in the figure (8). It can be noticed from the figure that the velocity and concentration profiles decrease with the increase of Lewis number Le .

Figure (9) concerns with the effect of Schmidt number Sc on the concentration profile. The concentration profile decrease with an increase Sc . Physically it is true, since the increase of Sc means decrease of molecular diffusivity that results in decrease of concentration boundary layer. Hence, the concentration of species is higher for small values of Sc and lower for higher values of Sc .

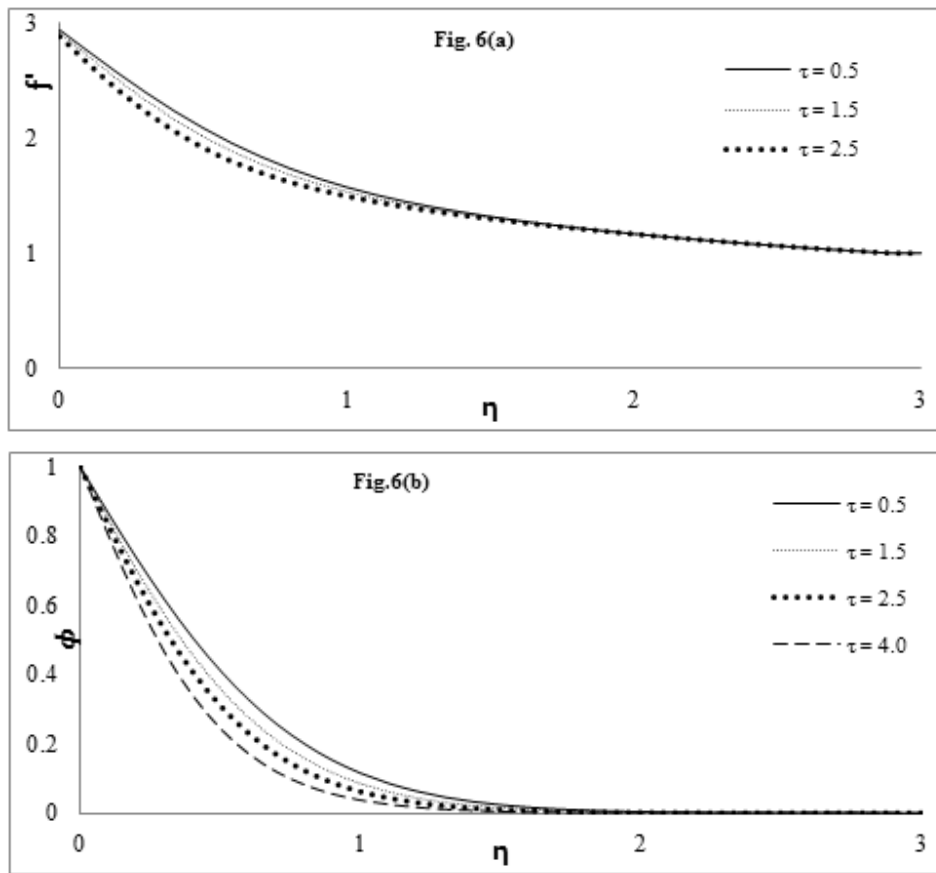
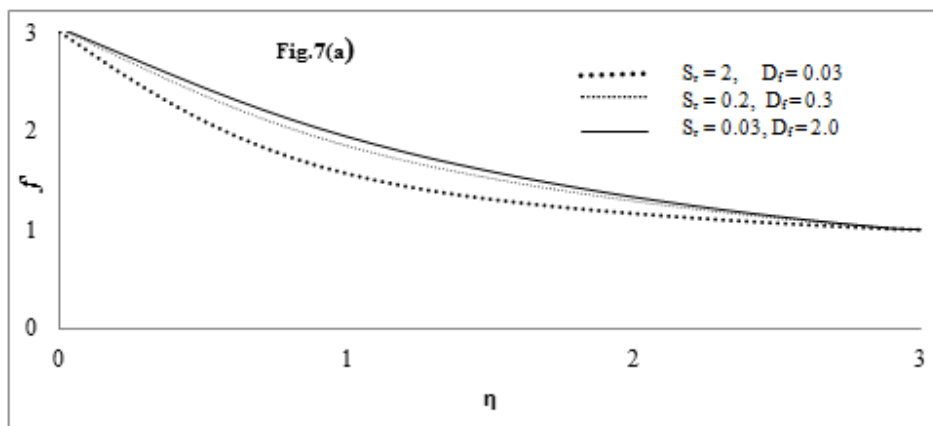


Fig.6 Effects of thermophoresis τ for $Ra_w/Pe_w=1$, $R = 0.5$, $\Lambda = 0.1$, $Pr = 0.73$, $Le = 2$, $Ha = 0$, $S_r = 2$, $D_f = 0.03$, $Sc = 1$, $N = 2$ and $Ec=0.5$ on (a) Velocity profile (b) Concentration profile

Figure (10) displayed the effect of Eckert number on the velocity, temperature and concentration profiles. It can be founded from figure velocity, temperature and concentration profiles increase with the increase of Eckert number Ec . This is because the Eckert number is the ratio of kinetic energy of the flow to the boundary layer enthalpy difference, The effect of viscous dissipation and flow fixed is to increase the energy, yielding a greater fluid temperature and as a consequence greater buoyancy force. The increasing buoyancy force due to an increase in the dissipation parameter enhances the temperature.



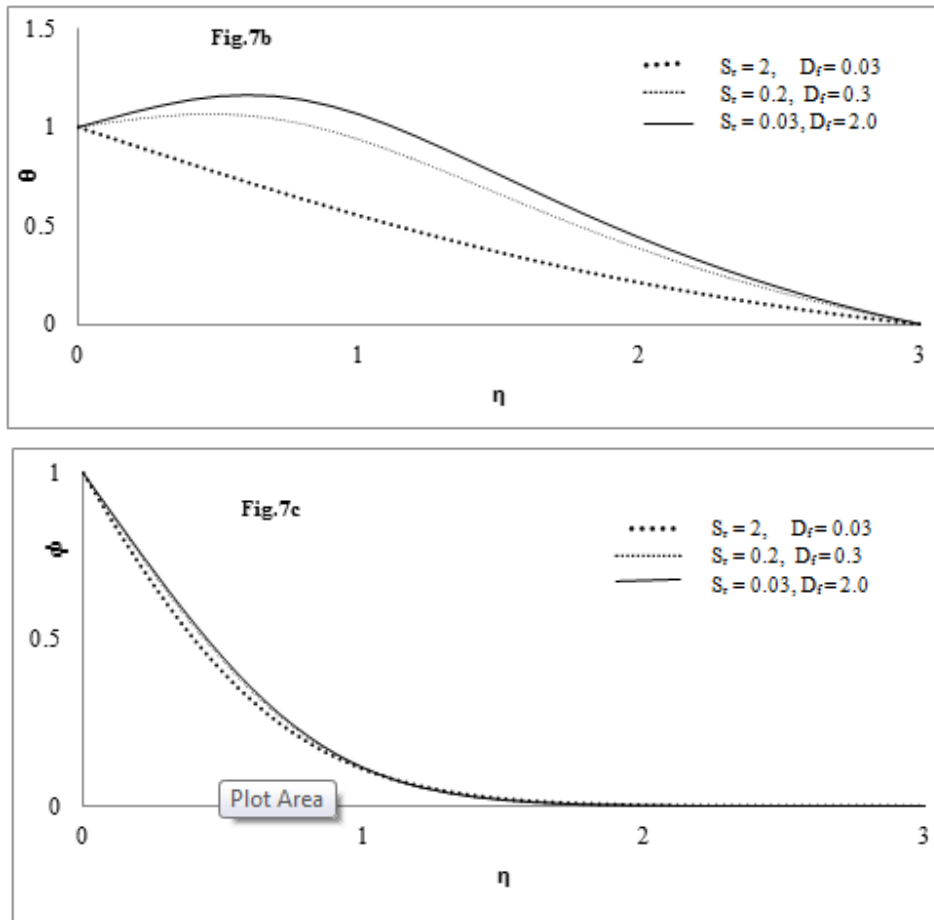
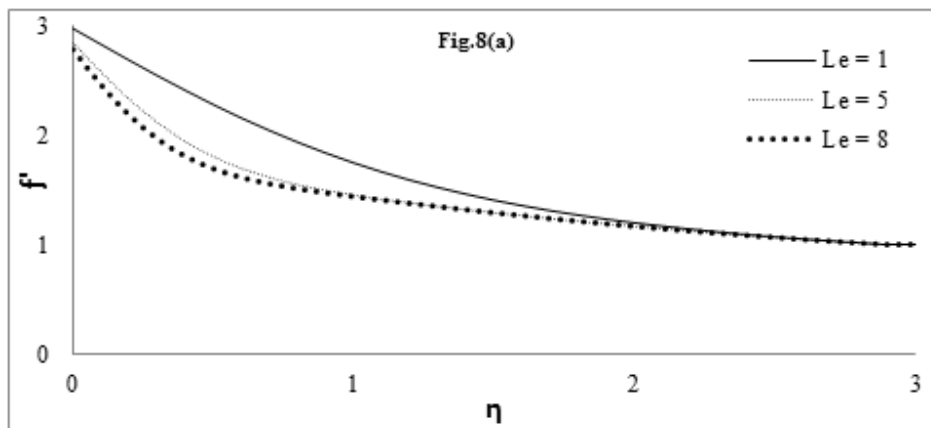


Fig.7 Effects of Soret and Dufour for $Ra_r/Pe_x=1$, $R = 0.5$, $\Lambda = 0.1$, $Pr = 0.73$, $Le = 2$, $Ha = 0$, $Sc = 1$, $N = 2$ and $Ec=0.5$ on (a) Velocity profile (b) Temperature profile (c) Concentration profile



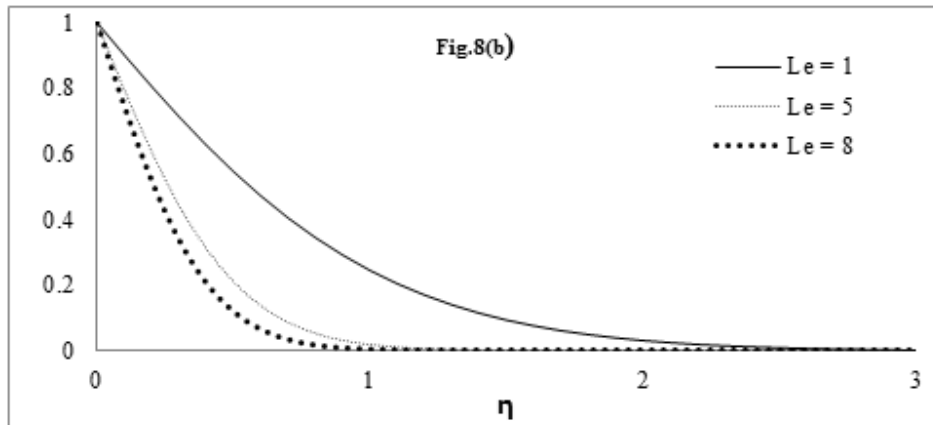


Fig. 8 Effects of Lewis number for $Ra_\nu/Pe_x=1, R = 0.5, A = 0.1, Pr = 0.73, Sc = 1, Ha = 0, S_r = 2, D_r = 0.03, \tau = 0.5, N = 2$ and $Ec=0.5$ on (a) Velocity profile (b) Concentration profile

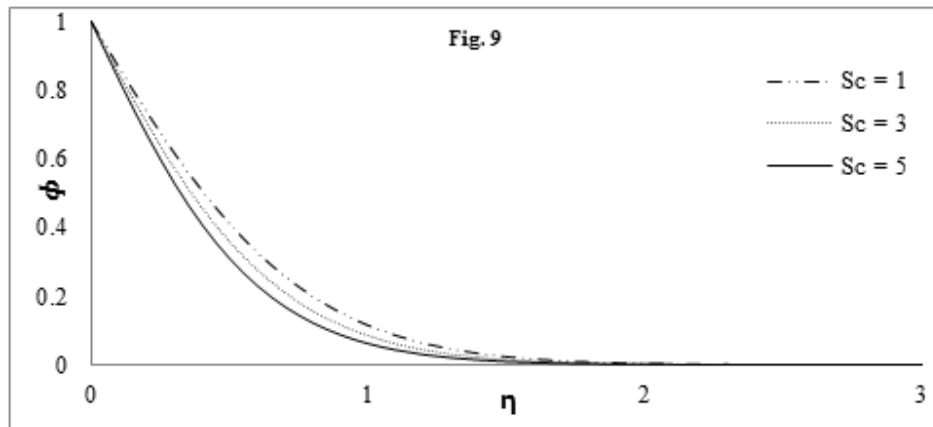
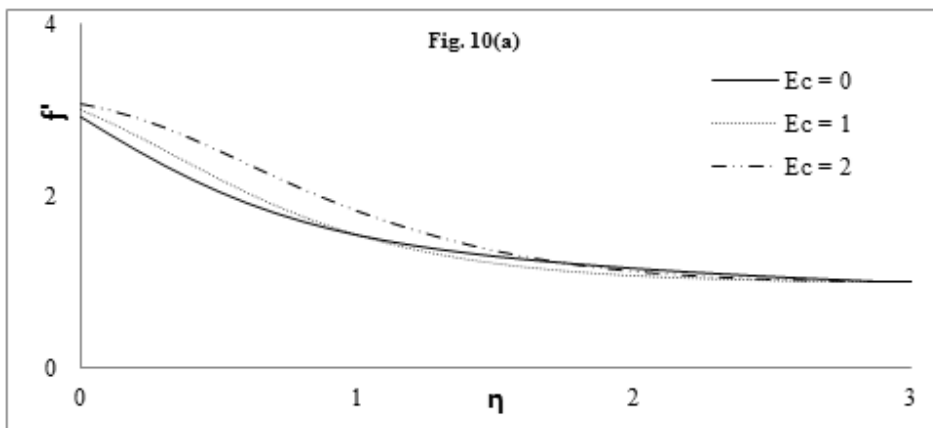


Fig. 9 Effects of Schmidt number Sc for $Ra_\nu/Pe_x=1, R = 0.5, A = 0.1, Pr = 0.73, Le = 2, Ha = 0, S_r = 2, D_r = 0.03, \tau = 0.5, N = 2$ and $Ec=0.5$ on Concentration profile



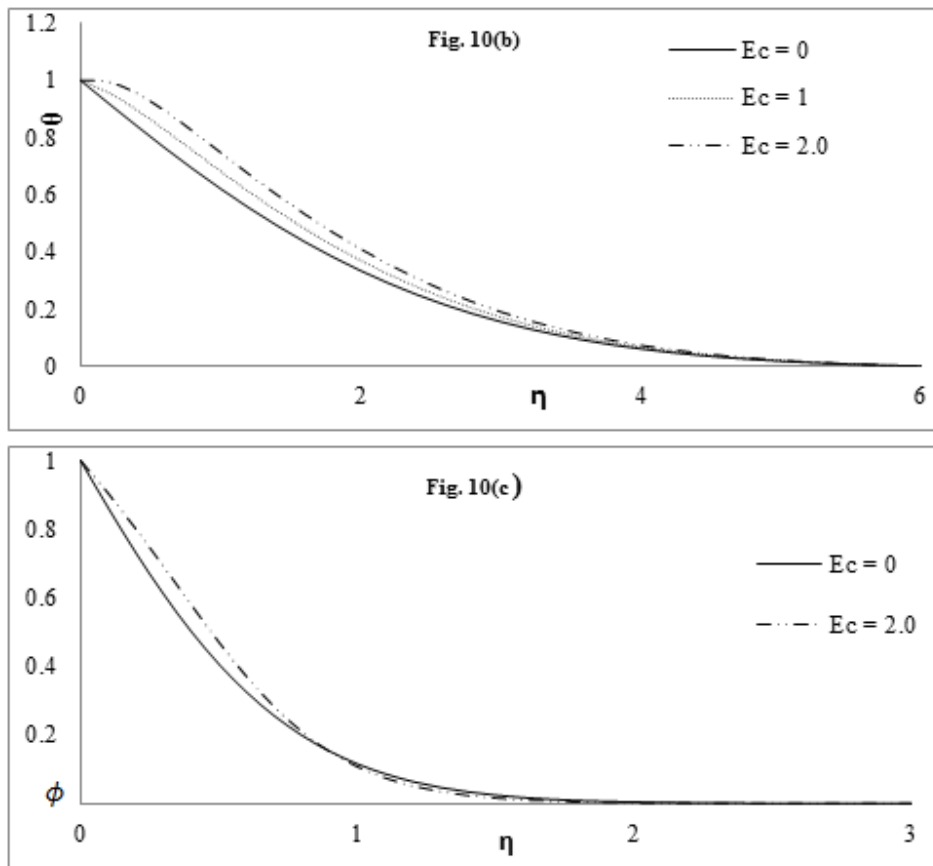


Fig. 10 Effects of Eckert number for $Ra_x/Pe_x=1$, $F=0.5$, $\Lambda=0.1$, $Pr=0.73$, $Le=2$, $Ha=0$, $Sc=1$, $\tau=0.5$, $N=2$, $S_r=2$, $D_f=0.03$ on (a) Velocity profile (b) Temperature profile (c) Concentration profile

REFERENCES

- [1]. EL-Kabeira SMM, Rashada AM and Rama Subba Reddy Gorla, *Mathematical and Computer Modelling*, **2007**, Vol.46, pp 384-397.
- [2]. Srinivasacharya D, Pranitha J. and RamReddy Ch, *International Journal of Nonlinear Science*, **2010**, 10(1), pp.61-69.
- [3]. Takhar H. S., Soundalgekar V. M and Gupta A. S., *International Journal of non-Linear Mechanics*, **1990**, Vol. 25, pp. 723-728,.
- [4]. Seddeek M. A., *International Communications in Heat and Mass Transfer*, **2005**, Vol. 32, pp. 258-265.
- [5]. Salem A.M, *Journal of the Korean Physical Society*, **2006**, Vol. 48(3), pp.109-113.
- [6]. Rami Y.J., fawzi A. and Abu-Al-Rub F., *Int.J.Numer. Methods Heat Fluid Flow*, **2001**, Vol. 11, pp. 600-618.
- [7]. Goren S.L, *J. Colloid Interface Sci.* **1977**, Vol. 61,.
- [8]. Gebhart B, *Journal of Fluid Mechanics*, **1962**, 14, pp. 225,
- [9]. Goldsmith P, and May F.G., Diffusiophoresis and thermophoresis in water vapour systems, in: C.N. Davies (Ed.), *Aerosol Science*, Academic Press, London, pp. **1966**, 163-194.
- [10]. Selim A., Hossain M.A. and Rees D.A.S., *Int. J. Thermal Sci.*, **2001**, 42, 973-982.
- [11]. Chamka A., Jaradat M. and Pop, *Int. J. Appl. Mech. Eng.*, **2004**, Vol.9, pp. 471-481,.
- [12]. Hossain M.A. and Takhar H. S., *Heat Mass Transf*, **1996**, Vol. 31, pp.243-248,.
- [13]. Damesh R. A, Duwairi H.M. and Al-Odat M., *Turk J Eng Environ Sci*, **1998**, Vol.30, pp. 83-89.
- [14]. Eckert E.R.G, and R.M. Drak, *Analysis of Heat and Mass Transfer*, McGraw-Hill, New York, 1972.
- [15]. Eldabe N. T., El-Saka A. G., and Ashraf Fouad, "Thermal-diffusion and diffusionthermo effects on mixed free-forced convection and mass transfer boundary layer flow for non-Newtonian fluid with temperature dependent viscosity" March **2008**, Vol.1, pp. 959-961,.

- [16] Srinivasacharya D. and RamReddy Ch., *Nonlinear Analysis Modeling and Control*, **2011**, Vol.16, No.1, pp. 100-115,.
- [17]. Kishan N. and Srinivas M., Thermophoresis and viscous dissipation effects on Darcy-Forchheimer MHD mixed convection in a fluid saturated porous media, **2012** Vol.3(1), pp.60-74,
- [18] Kakac S. and Yener Y, Convective Heat Transfer, Second edition, *CRC Press*, Florida, **1995**.
- [19] Rohsenow W.M., Hartnett J.P. and Cho Y.I, *Handbook of Heat Transfer*, McGraw-Hill, New York
- [20] Quinn Brewster M, *Thermal Radiative Transfer and Properties* John Wiley and Sons, New York, **1992**.
- [21] Raptis A., *Int. J. Heat Mass Transfer*, **1998**. Vol.41, pp. 2865-2866,
- [22]. Bellman R.B and Kalaba R.E., *Quasi-linearization and Non-Linear boundary value problem*, *Elsevier*, Newyork, **1965**.